Journal for ImmunoTherapy of Cancer

Enhanced efficacy of direct immunochemotherapy for hepatic cancer with image-guided intratumoral radiofrequency hyperthermia

Xuefeng Kan,[1,2] Guanhui Zhou,[1,3] Feng Zhang,[1] Hongxiu Ji,[1,4] David S Shin,[1] Wayne Monsky,[1] Chuansheng Zheng,[2] Xiaoming Yang [1]

To cite: Kan X, Zhou G, Zhang F, *et al*. Enhanced efficacy of direct immunochemotherapy for hepatic cancer with image-guided intratumoral radiofrequency hyperthermia. *Journal for ImmunoTherapy of Cancer* 2022;**10**:e005619. doi:10.1136/jitc-2022-005619

► Additional supplemental material is published online only. To view, please visit the journal online (http://dx.doi.org/10.1136/jitc-2022-005619).

XK and GZ contributed equally.

Accepted 05 November 2022

For numbered affiliations see end of article.

Correspondence to
Professor Xiaoming Yang; xmyang@uw.edu

Professor Chuansheng Zheng; hqzcsxh@sina.com

ABSTRACT

Background It is still a challenge to prevent tumor recurrence post radiofrequency ablation (RFA) of medium-to-large hepatocellular carcinomas (HCC). Immunochemotherapy, a combination of immunotherapy with chemotherapy, has demonstrated a great potential in augmenting the treatment efficacy for some malignancies. In this study, we validated the feasibility of using radiofrequency hyperthermia (RFH)-enhanced intratumoral immunochemotherapy of LTX-315 with liposomal doxorubicin for rat orthotopic HCC.

Methods Different groups of luciferase-labeled rat HCC cells and rat orthotopic HCC models were treated by: (1) phosphate buffered saline; (2) RFH; (3) LTX-315; (4) RFH+LTX-315; (5) liposomal doxorubicin; (6) RFH+liposomal doxorubicin; (7) LTX-315+liposomal doxorubicin; and (8) RFH+LTX-315+liposomal doxorubicin. Cell viabilities and apoptosis of different treatment groups were compared. Changes in tumor sizes were quantified by optical and ultrasound imaging, which were confirmed by subsequent histopathology. The potential underlying biological mechanisms of the triple combination treatment (RFH+LTX-315+liposomal doxorubicin) were explored.

Results Flow cytometry and MTS assay showed the highest percentage of apoptotic cells and lowest cell viability in the triple combination treatment group compared with other seven groups ($p<0.001$). Tumors in this group also presented the most profound decrease in bioluminescence signal intensities and the smallest tumor volumes compared with other seven groups ($p<0.001$). A significant increase of $CD8^+$ T cells, $CD8^+$/interferon (IFN)-γ^+ T cells, $CD8^+$/tumor necrosis factor (TNF)-α^+ T cells, and natural killer cells, and a significant decrease of regulatory T cells were observed in the tumors ($p<0.001$). Meanwhile, a significantly higher level of Th1-type cytokines in both plasma (interleukin (IL)-2, IL-12, IL-18, IFN-γ) and tumors (IL-2, IL-18, IFN-γ, TNF-α), as well as a significantly lower Th2-type cytokines of IL-4 and IL-10 in plasma and tumor were detected.

Conclusions Intratumoral RFA-associated RFH could enhance the efficacy of immunochemotherapy of LTX-315 with liposomal doxorubicin for HCC, which may provide a new strategy to increase the curative efficacy of thermal ablation for medium-to-large HCC.

WHAT IS ALREADY KNOWN ON THIS TOPIC

⇒ Hyperthermia induced by some sources can enhance immunotherapy in some preclinical cancer models, such as pancreatic cancer. LTX-315 in combination with doxorubicin showed therapeutic benefit in breast cancer.

WHAT THIS STUDY ADDS

⇒ Direct immunochemotherapy of LTX-315 in combination with liposomal doxorubicin is effective in the treatment of rat hepatocellular carcinoma. Radiofrequency hyperthermia significantly enhances the effect of direct immunochemotherapy (LTX-315+liposomal doxorubicin) on rat hepatocellular carcinoma.

HOW THIS STUDY MIGHT AFFECT RESEARCH, PRACTICE OR POLICY

⇒ The concept of this study may open new avenues for reducing the rates of residual and recurrent tumors after radiofrequency ablation of medium-to-large hepatocellular carcinomas.

INTRODUCTION

Although radiofrequency ablation (RFA) has become an effective alternative to surgery for management of early-stage hepatocellular carcinoma (HCC),[1] there is still a high incidence of tumor recurrence at the ablation zone margin, especially for medium-to-large tumors (>3 cm).[2] Attempts have been made to address this challenge, such as RFA combined with transarterial chemoembolization.[3] However, the local tumor progression rate in medium-to-large HCCs is still up to 30.4% after such combination treatment.[4] Thus, there is a pressing clinical need to develop more effective treatment strategies to target the residual tumor cells following RFA, and thereby improve the long-term survival of these patients.

Systemic therapy is recommended for advanced HCC according to Barcelona

Clinic Liver Cancer staging.[5] However, some randomized controlled trials failed to show overall survival benefit of various chemotherapeutic regimens.[6] Furthermore, high-dose chemotherapy often results in toxicity and resistance. One approach to improve the efficacy of traditional chemotherapy is to capsulate chemotherapeutics. For example, liposomal doxorubicin enables a long-term release of doxorubicin from liposome shells, allows for accumulation in tumors, and reduces undesirable systemic side effects of doxorubicin.[7 8] Meanwhile, there is a growing focus on a new treatment approach using low-dose or medium-dose chemotherapeutics at short repeated intervals to activate antitumor immunity while selectively depleting immunosuppressive cells, such as regulatory T cells (Tregs).[9] Furthermore, it was reported that doxorubicin can induce immunogenic cell death and inhibit immunosuppressive cells,[10 11] thereby eliminating the obstacles implemented on the immune system by such cells.

In recent years, the emergence of new immunotherapies, such as immune checkpoint blockade, chimeric antigen receptor T cell therapies, and oncolytic viruses, has presented additional potential therapeutic options for advanced HCC.[12 13] However, the response rate to these treatments has been low so far, primarily due to the formation of an immunosuppressive microenvironment.[14] The combination of immunotherapy with other therapeutic methods may enhance the antitumor efficacy.[15 16] Immunochemotherapy, a combination of immunotherapy with chemotherapy, has demonstrated a great potential in augmenting the treatment efficacy for some malignancies, such as lung cancer, esophageal cancer, and large B cell lymphoma.[17–19]

LTX-315, a first-in-class oncolytic peptide, can kill cancer cells by a membranolytic effect on the cellular plasma membrane and intracellular organelles, such as mitochondria, golgi complex, and lysosomes, which further leads to a subsequent release of danger-associated molecular pattern molecules and tumor antigens that recruit and activate T cells for immunotherapy.[20 21]

Previous studies have demonstrated that radiofrequency hyperthermia (RFH) at approximately 42°C can significantly enhance the effect of chemotherapy or oncolytic immunotherapy (such as LTX-401) effect on a variety of malignancies.[22–25] The potential mechanisms may include (1) RFH-induced modulation of the tumor immune microenvironment via heat shock proteins and subsequent activation of immune systems[26]; (2) tissue fracturing by heating, increased permeability of the cytoplasmic membrane, deactivation of multidrug resistance pumps, and amplification of cellular metabolism, which facilitate the entrance of therapeutics into the targeted tumor cells.[27]

In the present study, LTX-315 was used to kill HCC cells, and subsequently recruit and activate T cells for immunotherapy. Liposomal doxorubicin was used to improve immunosuppressive microenvironment of HCC by reducing Tregs. RFH was used to enhance the treatment efficacy of LTX-315 and liposomal doxorubicin. The purpose of the present study was attempted to fully combine and apply, at the first time, the advantages of three advanced image-guided therapy, including oncolytic immunotherapy, chemotherapy, and RFH, to explore a new strategy, so-called 'interventional triple treatment', for more effective management of HCC, one of the most common malignancies worldwide.

MATERIALS AND METHODS

Study design

This study included two phases: (a) in vitro demonstration of the synergistic therapeutic effect of LTX-315 (MedChemExpress, New Jersey, USA) with liposomal doxorubicin (Distributed by Dr. Reddy's Laboratories, Princeton, New Jersey, USA, Made in India, 2 mg/mL) on HCC cells with and without RFH; and (b) in vivo validation of the technical feasibility of RFH-enhanced therapeutic effect with LTX-315 plus liposomal doxorubicin in animal models with orthotopic HCCs.

In vitro experiments

Cell culture

McA-RH7777 cells (American Type Culture Collection, Manassas, Virginia, USA) were transfected with lentiviral luciferase/red fluorescence protein (Luc/RFP) genes to create Luc/RFP-positive HCC cells (GeneCopoeia, Rockville, Maryland, USA). The Luc/RFP-positive McA-RH7777 cells were sorted using fluorescence-activated cell sorting technique (Aria II, Becton Dickinson, Franklin Lakes, New Jersey, USA) and cultured in Dulbecco's Modified Eagle's Medium (Life Technologies, Carlsbad, California, USA) supplemented with 10% fetal bovine serum at 37°C in a humidified atmosphere containing 5% carbon dioxide. For statistical analysis, each in vitro cell experiment was repeated six times.

Determination of 50% inhibitory concentrations of LTX-315 and liposomal doxorubicin for rat HCC cells

Luc/RFP-positive McA-RH7777 cells were seeded in a 96-well plate at a density of 1×10^4 cells per well in 100 µL cell culture medium. LTX-315 and liposomal doxorubicin at various concentrations were added to the wells and incubated for 24 hours. MTS assay was used to examine cell viability. Briefly, 10 µl MTS reagent was added into each cell, and then cells were incubated at 37°C for 4 hours. The absorbance was detected at 490 nm with a Microplate Reader (VersaMax; Molecular Devices, Sunnyvale, California, USA). A non-linear regression was used to calculate the 50% inhibitory concentrations (IC50) of LTX-315 and liposomal doxorubicin. The IC50 doses of LTX-315 and liposomal doxorubicin were used for Luc/McA-RH7777 cell treatment in the following in vitro experiments.

RFH-enhanced cytotoxic effect of LTX-315 and liposomal doxorubicin in HCC cells

Luc/RFP-McA-RH7777 cells were divided into the following eight treatment groups: (1) phosphate buffered

saline (PBS); (2) 30 min RFH at 42ºC alone; (3) LTX-315 alone; (4) LTX-315 plus 30 min RFH at 42ºC; (5) liposomal doxorubicin alone; (6) liposomal doxorubicin plus 30 min RFH at 42ºC; (7) LTX-315 plus liposomal doxorubicin; and (8) triple combination treatment with LTX-315 and liposomal doxorubicin, immediately followed by 30 min RFH at 42ºC. RFH was performed as previously described.[23 28]

Twenty-four hours after treatments, a cell suspension at density of 1×10^6 mL was made by digestion with 0.25% trypsin without EDTA, followed by PBS washing and resuspension in 200 µL binding buffer. Subsequently, 5 µL annexin V-FITC (BD Biosciences, San Diego, California, USA) and 5 µL 7-Amino-Actinomycin D (BD Biosciences) were added and incubated for 10 min. Then, flow cytometry was used to quantify the necrotic/apoptotic cells. The data were analyzed by FloJo Data Analysis Software (V.10; Ashland, Oregon, USA).

Cells viability was evaluated by the 3-(4,5-dimethylthiazol-2-yl)−5-(3-carboxymethoxyphenyl)−2-(4-sulfophenyl)−2H-tetrazolium (MTS) assay. The relative cell viability of each group was evaluated using the equation: $A_{treated} - A_{blank} / A_{control} - A_{blank}$, where A represents the absorbance.

Cells in culture chamber slides were washed two times with PBS, fixed with 4% paraformaldehyde, and then dried at room temperature. The cells were counterstained with 4', 6-diamidino-2-phenylindole (Southern-Biotech, Birmingham, Alabama, USA) and imaged with a fluorescent microscope (IX73, Olympus, Tokyo, Japan).

Bioluminescence optical imaging of treated cells

Fluorescent signal intensity (SI) of treated cells was evaluated 24 hours after the treatment. Cells in each of eight groups were collected and suspended in 200 µL PBS, followed by adding 5 µL of Pierce D-Luciferin (Thermo Fisher Scientific, Rockford, Illinois, USA). The suspension was transferred to cylindrical glass tubes. Bioluminescence optical imaging was performed using an imaging system (In-Vivo Xtreme; Bruker, Billerica, Massachusetts, USA). Bioluminescence SI was quantified as the sum of all detected photon counts. Data were normalized to relative signal intensity (RSI) by using the following equation: $RSI=SI_T/SI_C$, where SI represents signal intensity, T represents the treatment group, and C represents the control group.

In vivo experiments

Creation of rat model with orthotopic hepatic cancer

The animal experiments were approved by our institutional Animal Care and Use Committee (No: 4120–02). An orthotopic hepatic cancer model was created in Sprague-Dawley rats (Charles River, Hollister, California, USA), which weighed 200–250 g. To prevent spontaneous tumor regression of McA-RH7777 tumors, cyclosporine A (20 mg/kg/day; Novartis Pharma Stein AG, Stein, Switzerland) was subcutaneously administrated from one day before the tumor implantation through day 4 after the tumor implantation.[29 30] Under anesthesia with 1–3% isoflurane (Piramal Healthcare, Andhra Pradesh, India) delivered in the inhalation of 100% oxygen and using an aseptic technique, the liver was exposed through a subxiphoid abdominal incision. Subsequently, $0.5–1\times10^7$ Luc/RFP-positive McA-RH7777 cells mixed in 50 µL of PBS and 50 µL of Matrigel (Discovery Labware, Bedford, Massachusetts, USA) were inoculated into the left lobe of the liver, followed by 5 min of compression of cell injection site with a gelatin sponge (Pharmacia & Upjohn, Division of Pfizer, New York, USA). The abdominal incision was closed with layered sutures.

RFH-enhanced therapy of LTX-315 and liposomal doxorubicin for rat orthotopic HCCs

Forty-eight rats with orthotopic hepatic cancers were randomly assigned into eight treatment groups (n=6/group): (1) intratumoral injection of 100 µL PBS; (2) intratumoral RFH (42°C for 30 min) alone; (3) intratumoral injection of 1.0 mg LTX-315 in 100 µL of PBS alone; (4) intratumoral injection of 1.0 mg LTX-315 in 100 µL of PBS, followed by intratumoral RFH; (5) intratumoral injection of 1 mg/kg liposomal doxorubicin alone; (6) intratumoral injection of 1 mg/kg liposomal doxorubicin, followed by intratumoral RFH; (7) intratumoral injection of 1.0 mg LTX-315 in 100 µL PBS and 1 mg/kg liposomal doxorubicin; and (8) triple combination treatment with intratumoral injection of 1.0 mg LTX-315 in 100 µL PBS and 1 mg/kg liposomal doxorubicin, followed by intratumoral RFH.

The intratumoral RFH with LTX-315 and liposomal doxorubicin injection was performed by precisely deploying a multiprong RFA electrode in tumor periphery under real-time ultrasound imaging guidance. A hamilton microsyringe was used for injection of therapeutic agents at a rate of 100 µL per 3 min. The electrode was connected to an RFA generator (WE7568-II, Welfare Electronics) to deliver thermal energy to the tumors at approximately 42°C for 30 min. The methods on measuring and controlling the temperature during RFH were detailed in previous studies.[22 23]

Optical and ultrasound imaging to assess tumor growth

Optical imaging was used to assess treatment response using the in vivo imaging system (Bruker) one day before treatment, as well as days 7 and 14 after the treatment. Optical images were acquired 20 min after the intraperitoneal administration of D-luciferin at 150 mg/kg. RSI was calculated using the equation: $RSI=SI_{Dn}/SI_{D0}$, where SI represents signal intensity, Dn represents day n after treatment, and D0 represents the day before treatment.

Contrast-enhanced ultrasound imaging was performed to follow-up the tumor growth 1 day before treatment, as well as 7 and 14 days after treatment. The tumor volume at axial, longitudinal, and depth diameters was calculated according to the following equation: $v=x\times y\times z\times\pi/6$. Data were expressed as relative tumor volume (RTV) by using the following equation: $RTV=V_{Dn}/V_{D0}$, where V represents

tumor volume, Dn represents the day n after treatment, and D0 represents the day before treatment.

Pathologic correlation/confirmation

Tumors were harvested respectively 2 weeks after the treatments. The samples were fixed with 4% paraformaldehyde, embedded in paraffin, and sectioned at 4 µm thickness. Six histology sections were assessed per tumor. Tissue sections were analyzed with H&E staining, terminal deoxynucleotidyl transferase dUTP nick end labeling (TUNEL) staining, and Ki-67 staining. The tumor necrosis rate was computed by the area percentage of the necrotic region in the total tumor, which was calculated from H&E staining sections as follows: tumor necrosis rate (%)=N/(N+T), where N represents the necrotic area of the tumor, and T represents non-necrotic area of the tumor.[31 32] The spatial orientation of necrotic regions after each different treatment was mainly in the center of tumor.

Different immunohistochemical staining techniques, including CD8 for $CD8^+$ T cells, ANK61 for natural killer (NK) cells, and Foxp3 for Tregs were performed to analyze immune cell infiltration among different treatment groups.

Flow cytometry analysis of tumor tissues

Tumors were digested to prepare cell suspensions with collagenase and hyaluronidase solution. Then, the cell suspensions were filtered through a cell mesh (70 µm, BD Biosciences). The antibodies to CD45 (clone OX-1), CD3 (clone G4.18), CD4 (clone OX-35), CD8 (clone OX-8), NKR-P1A (clone 10/78), FoxP3 (clone FJK-16s), IFN-γ (clone DB-1), and TNF-α (clone TN3-19.12) were obtained from BD Biosciences. For intracellular cytokine staining, the harvested cells were stimulated with PMA (50 ng/mL) and ionomycin (500 ng/mL) for 4 hours and incubated for 1 hour with brefeldin A (10 µg/mL). Then, the cells were permeabilized using an Foxp3 Fixation and Permeabilization Kit (BD Bioscience). Subsequently, Foxp3, IFN-γ, and TNF-α were stained. Flow cytometric analysis was performed using the FACS flow cytometer (LSRFortessa X-20, BD). The data were analyzed by FloJo Data Analysis Software (V.10; Ashland, Oregon, USA).

ELISA assay and quantitative real-time PCR

Blood was collected via the tail vein into tubes containing EDTA. Plasma was obtained by centrifugation at 1000 g for 10 min and stored at −70°C until analysis. Concentrations of interleukin (IL)-2, IL-4, IL-10, IL-12, IL-18, and interferon (IFN)-γ in plasma were measured by ELISA using High Sensitivity ELISA Kit (eBiosciences).

Tumors in all groups were collected and stored in RNA Later (Servicebio, CFX) at −20°C. Total RNA was extracted from tumors using Qiagen RNeasy Mini Kit (Qiagen, Germany) and complementary DNA (cDNA) was synthesized using iScript Reverse Transcription Supermix (Bio-Rad, Hercules, California, USA). Subsequently, cDNA was used to measure the messenger RNA level of IL-2, IL-4, IL-18, tumor necrosis factor (TNF)-α, IFN-γ, IL-10 by quantitative real-time PCR (qRT-PCR) using the ABI Viia7 RT-PCR System (Applied Biosystems). All the sequences of primers are listed in online supplemental table S1. A housekeeping gene GAPDH was used as an internal control. The relative quantification was performed with the comparative threshold cycle method as described by the manufacturer.

Statistical analysis

The non-linear regression analysis for IC50 determination was performed using GraphPad Prism V.8.0.1 (San Diego, California, USA). A two-tailed independent samples t-test with equal variance was used to compare cell apoptosis, cell viability, relative photo signal, RTV, relative tumor weight, tumor necrosis rate, TUNEL IOD sum, KI67 IOD sum, CD8 cells per 400×field, AKN61 IOD sum, Foxp3 IOD sum, percentages of different immune cells subtypes in tumor tissues, and levels of different cytokines in plasma and tumors between two different groups. One-way analysis of variance with the Dunnett t-test was used to compare these factors above between the triple treatment (RFH+LTX-315+liposomal doxorubicin) group and each of the other groups. Statistical analysis was carried out using SPSS V.24.0 software (Chicago, Illinois, USA). P value <0.05 was considered statistically significant.

RESULTS

In vitro experiments

The IC50 of LTX-315 and liposomal doxorubicin for rat HCC cells

Both LTX-315 and liposomal doxorubicin showed dose-dependent anti-proliferative effects on Luc/RFP-positive McA-RH7777 cells. The IC50 value of LTX-315 was 40.98 µg/mL, and the IC50 value of liposomal doxorubicin was 2.207 mg/mL for McA-RH7777 cells.

Comparison of cytotoxic effects among different treatment groups

Apoptosis analysis by flow cytometry demonstrated significantly higher percentages of necrotic/apoptotic cells in (1) cells treated with RFH+LTX-315 than in those treated with LTX-315 alone; (2) cells treated with RFH+liposomal doxorubicin than in those treated with liposomal doxorubicin alone; and (3) cells treated with LTX-315+liposomal doxorubicin than in those treated with either LTX-315 or liposomal doxorubicin alone. The highest percentage of necrotic/apoptotic cells was observed in the group treated with the triple combination treatment (RFH+LTX-315+liposomal doxorubicin) in comparison to other seven treatment groups (figure 1A,B, online supplemental table S2). The MTS assay further confirmed that the viability of cells was significantly lower in (1) the group treated with RFH+LTX-315 compared with the group treated with LTX-315 alone; (2) the group treated with RFH+liposomal doxorubicin compared with the group treated with liposomal doxorubicin alone; and (3) the group treated with LTX-315+liposomal doxorubicin compared with LTX-315 or liposomal doxorubicin alone. The lowest viability of cells was observed in the triple combination

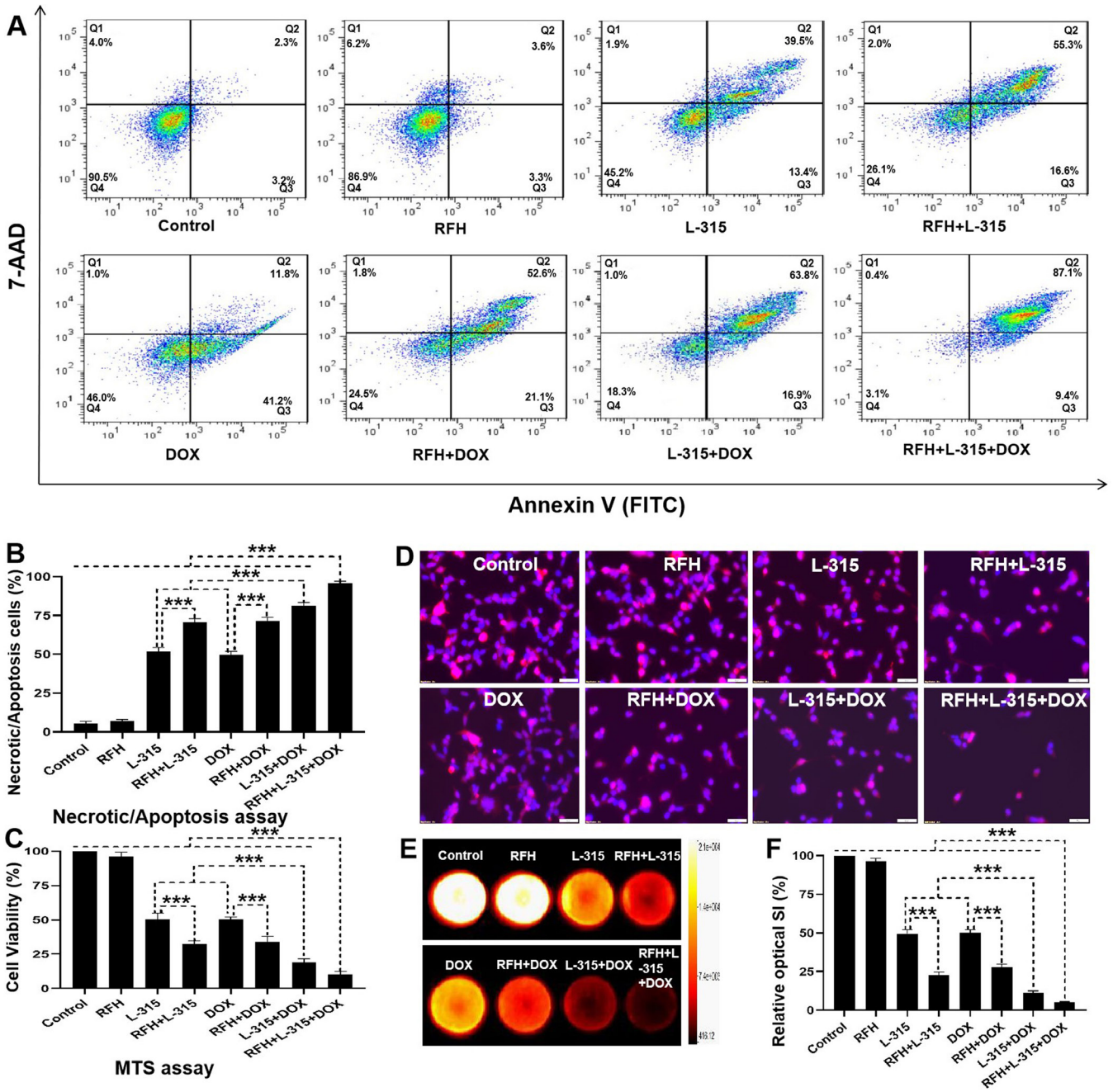

Figure 1 Flow cytometry, MTS assay, fluorescent microscopy, and bioluminescence optical imaging of the treated hepatocellular carcinomas cells. (A, B) Twenty-four hours after the treatment, flow cytometry shows significantly higher percentage of necrotic/apoptotic cells in the triple combination treatment group (RFH+LTX-315 (L-315)+DOX) in comparison to other seven groups (***p<0.001). (C) Twenty-four hours after the treatment, MTS assay demonstrates significantly lower cell viability in the triple combination treatment group, compared with other seven treatment groups (***p<0.001). (D) Twenty-four hours after the treatment, fluorescent microscopy shows fewer survival cells in the triple combination treatment group (Scale bars, 50 µm), while optical imaging (E, F) demonstrates the lowest relative fluorescent signal in the triple combination treatment group, compared with other seven groups (***p<0.001). All the data are from a representative experiment repeated six times. Error bars represent SD. RFH, radiofrequency hyperthermia; SI, signal intensity; 7-AAD, 7-Amino-Actinomycin D.

treatment group compared with other seven treatment groups (figure 1C, online supplemental table S2).

Fluorescent microscopy performed 24 hours after the treatments showed fewer viable cells in the RFH+LTX-315 group compared with the LTX-315 alone group, in the RFH+liposomal doxorubicin group compared with the liposomal doxorubicin alone group, and in the LTX-315+liposomal doxorubicin group compared with either LTX-315 group or liposomal doxorubicin group. The fewest number of survival cells was seen in the triple combination treatment (RFH+LTX-315+liposomal doxorubicin) group compared with other seven groups (figure 1D). Bioluminescence optical imaging demonstrated a significantly lower relative bioluminescence

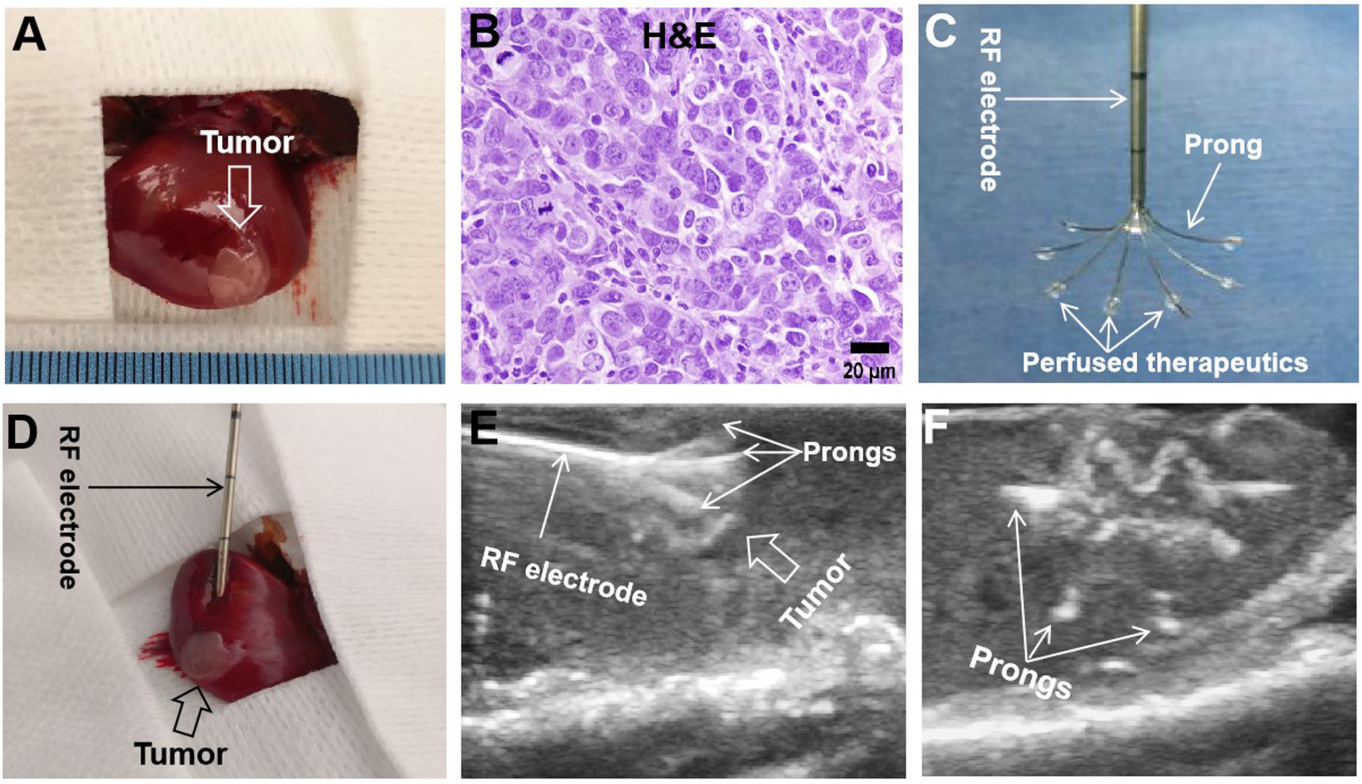

Figure 2 Creation of rat orthotopic hepatic cancer for radiofrequency hyperthermia-enhanced treatment. (A) At 7 days after tumor implantation, an orthotopic hepatic tumor (arrow) is created in the rat liver. (B) Tumors were harvested 2 weeks after the treatments. H&E staining confirms the hepatocellular carcinomas formation (obtained from the controlled group). (C) Tumors received the treatments at 7 days after tumor implantation. The multimodal perfusion-thermal radiofrequency (RF) ablation electrode permits simultaneous peritumoral infusion of therapeutics and generation of RF hyperthermia. (D–F) Under real-time ultrasound imaging guidance, the multimodal ablation electrode is placed into the tumor and then multiple prongs are precisely deployed to cover the entire tumor to deliver therapeutics, followed by intratumoral radiofrequency hyperthermia to further enhance the treatment efficacy.

signal in (1) the RFH+LTX-315 group than in the LTX-315 alone group; (2) the RFH+liposomal doxorubicin group than in the liposomal doxorubicin alone group; (3) the LTX-315+liposomal doxorubicin group than in either LTX-315 or liposomal doxorubicin alone groups. The lowest relative bioluminescence signal was observed in the group with triple combination treatment (figure 1E, F, online supplemental table S2).

Altogether, these results confirmed that LTX-315 in combination with liposomal doxorubicin has a better cell-killing effect on rat HCC cells compared with LTX-315 or liposomal doxorubicin alone. Additionally, RFH significantly enhances the cell-killing effect of LTX-315, liposomal doxorubicin, and LTX-315+liposomal doxorubicin on rat HCC cells.

In vivo experiments

Creation of rat orthotopic hepatic cancer

The orthotopic hepatic cancer was detected in the left lobes of rat livers 7 days after tumor implantation (figure 2A, B). No significant difference in average baseline tumor volume was found among the eight groups before treatment (p=0.999) (online supplemental table S3). Under ultrasound imaging guidance, a radiofrequency (RF) electrode was precisely placed in the tumor and multiple thermal infusion prongs were extended to cover the entire tumor for delivery of therapeutic agents, followed by delivery of RF-induced thermal energy to further enhance the treatment efficacy (figure 2C–F).

Optical and ultrasound imaging of rat orthotopic hepatic cancers in the eight groups

The follow-up assessment of treated rat hepatic tumors by bioluminescence optical imaging and contrast-enhanced ultrasound imaging, showed a significantly lower relative photon signal of tumors and a significantly smaller RTV treated with (1) RFH+LTX-315 compared with those treated with LTX-315 alone; (2) RFH+liposomal doxorubicin compared with those treated with liposomal doxorubicin alone; and (3) LTX-315+liposomal doxorubicin compared with those treated with LTX-315 alone or liposomal doxorubicin alone. The lowest relative photon signals and the smallest RTV were seen in tumors treated with RFH+LTX-315+liposomal doxorubicin compared with other seven treatment groups (figure 3, online supplemental table S3). Collectively, these in vivo results further confirmed the LTX-315 in combination with liposomal doxorubicin has a better treatment effect for rat

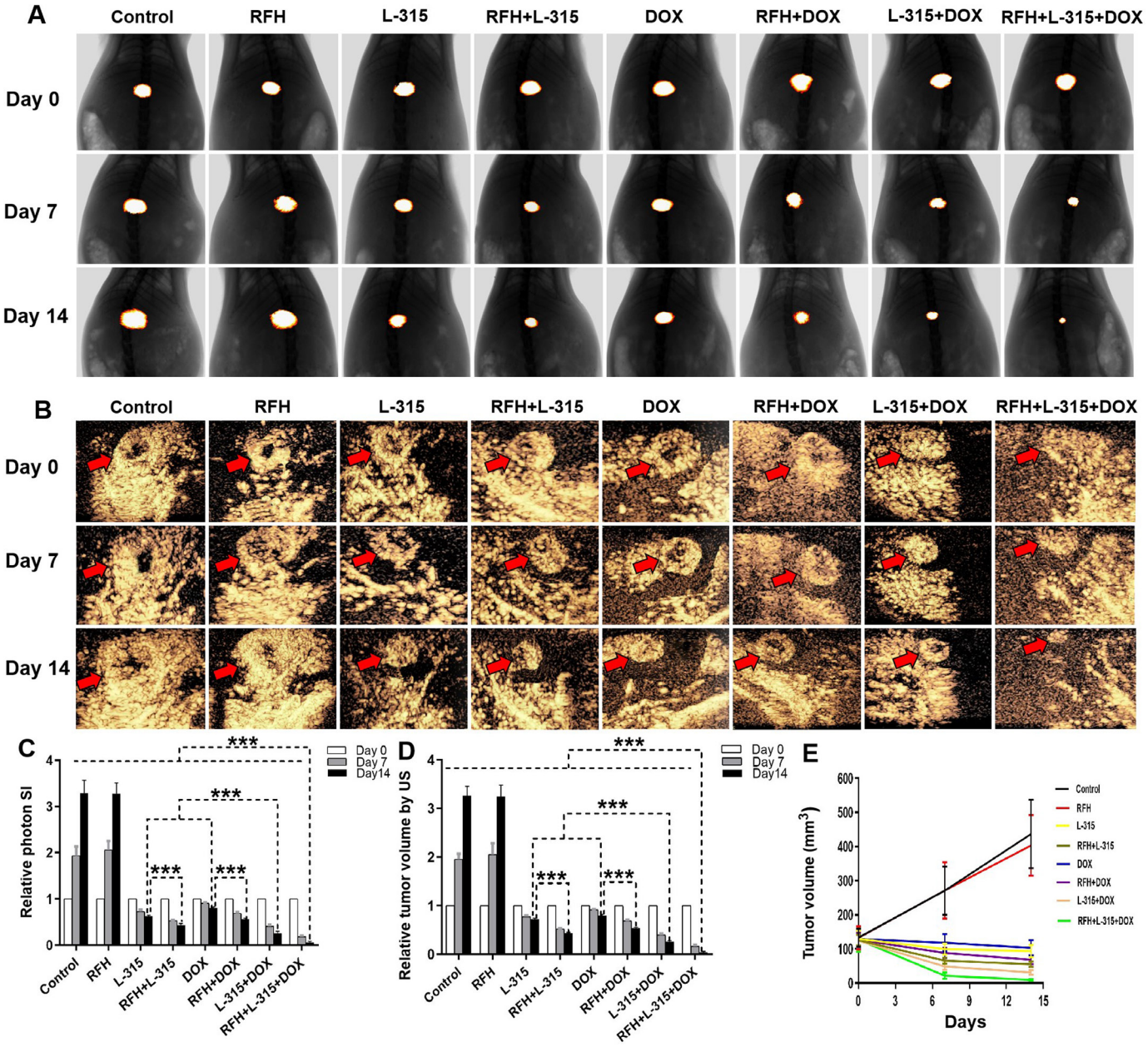

Figure 3 Optical/X-ray imaging and contrast-enhanced ultrasound imaging follow-up of treated tumors among eight animal groups. The Optical/X-ray imaging (A) and contrast-enhanced ultrasound imaging (B) shows the tumors (golden-yellow color, red arrows) presented with smaller tumor size in the triple combination treatment (RFH+LTX-315 (L-315)+DOX) group, compared with other seven treatment groups (***p<0.001). (C, D) The quantitative analysis shows a significantly lower relative optical signal intensity and smaller relative tumor volume in the triple combination treatment (RFH+LTX-315 (L-315)+DOX) group, compared with other seven treatment groups (***p<0.001). (E) Tumor growth chart shows the tumors in the triple combination treatment group with the smallest tumor size at 7 and 14 days after treatments, compared with other seven treatment groups. n=6 in each group. Error bars represent SD. RFH, radiofrequency hyperthermia; SI, signal intensity.

HCC compared with LTX-315 or liposomal doxorubicin alone, and the enhancement effect of RFH on LTX-315, liposomal doxorubicin, and LTX-315+liposomal doxorubicin for rat HCC.

Histology analysis

Tumors were harvested and weighed. A significantly lower relative tumor weight was demonstrated when treated with: (1) RFH+LTX-315 compared with LTX-315 alone; (2) RFH+liposomal doxorubicin compared with liposomal doxorubicin alone; (3) LTX-315+liposomal doxorubicin compared with LTX-315 alone or liposomal doxorubicin alone. The smallest relative tumor weight was noted in the triple combination treatment group (RFH+LTX-315+liposomal doxorubicin) compared with other seven groups (figure 4A,B, online supplemental table S4). Tumor necrosis analysis by H&E staining, apoptosis analysis by TUNEL staining, and cell proliferation analysis by Ki-67 staining corroborated the above

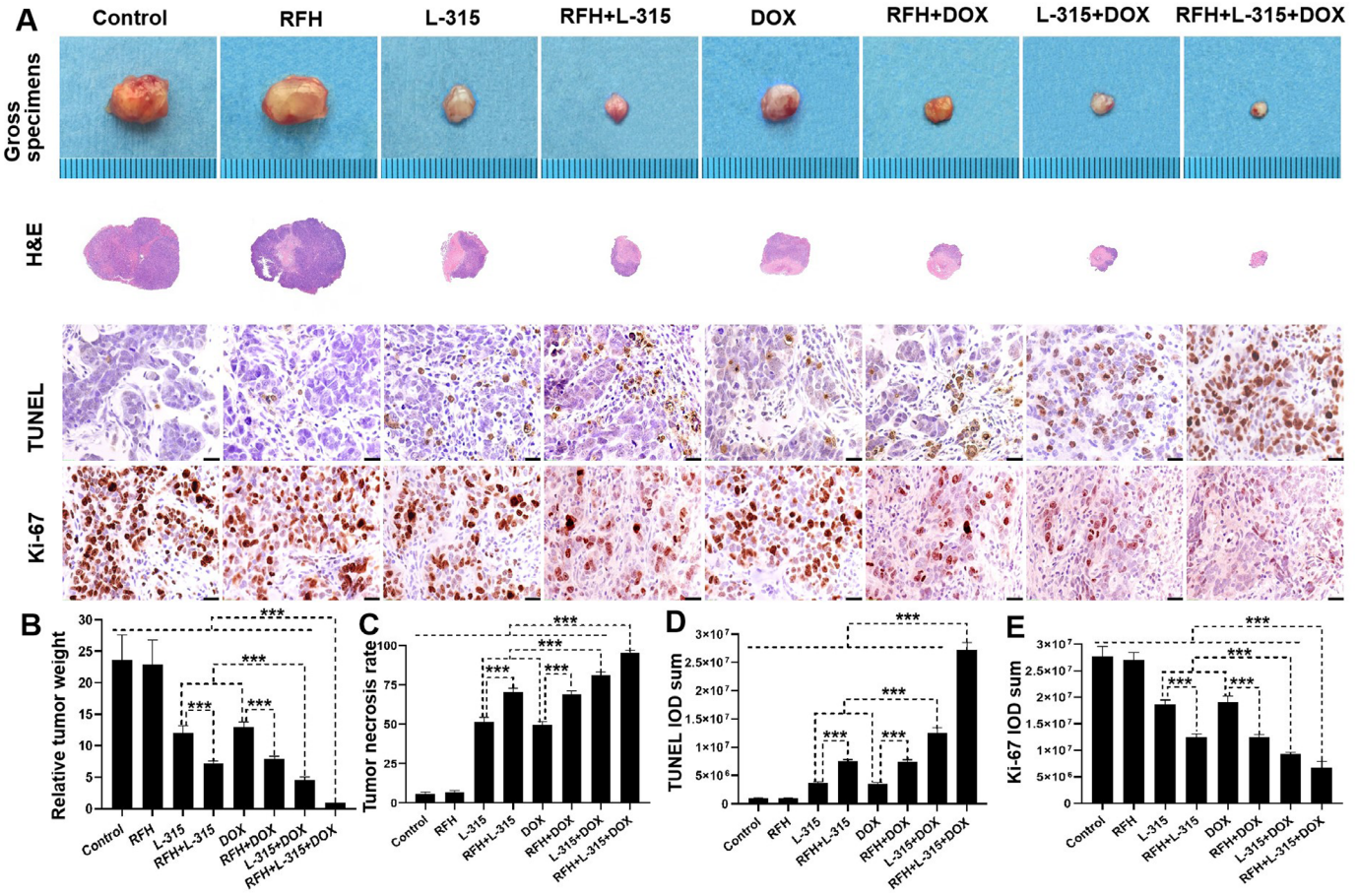

Figure 4 Pathologic analysis of the tumors in eight treatment groups. (A, B) Representative tumors harvested from different groups, showing the smallest tumor size/weight in the triple combination treatment (RFH+LTX-315 (L-315)+DOX) group, compared with other seven treatment groups (***p<0.001). (A, C–E) The H&E, TUNEL, and Ki-67 staining further confirms a significantly higher tumor necrosis rate, more apoptotic cells (yellow brown dots), and fewer proliferating cells (yellow brown dots) in the triple combination treatment, compared with other seven treatment groups (Scale bars, 20 µm) (***p<0.001). n=6 in each group. Error bars represent SD. RFH, radiofrequency hyperthermia; TUNEL, transferase dUTP nick end labeling.

findings with a significantly higher rate of tumor necrosis, more apoptotic cells, and fewer proliferating cells in (1) the RFH+LTX-315 group compared with the LTX-315 alone group; (2) the RFH+liposomal doxorubicin group compared with the liposomal doxorubicin alone group; and (3) the LTX-315+liposomal doxorubicin group compared with the LTX-315 alone group or liposomal doxorubicin alone group (figure 4A and C–E, online supplemental table S4). Significantly greatest number of apoptotic cells, least number of proliferation cells, and highest rate of tumor necrosis were found in the triple combination treatment (RFH+LTX-315+liposomal doxorubicin) group compared with other seven treatment groups (online supplemental table S4). These results further demonstrated the treatment effect of LTX-315 with liposomal doxorubicin, and the enhancement effect of RFH on LTX-315, liposomal doxorubicin, and LTX-315+liposomal doxorubicin for rat HCC.

As shown in figures 5 and 6, the immunohistochemistry analysis and flow cytometry analysis showed a significant increase of $CD8^+$ T cells, $CD8^+$/IFN-γ^+ T cells, $CD8^+$/TNF-α^+ T cells, NK cells, a significant decrease of Tregs, and a significantly higher ratio of pro-immune ($CD8^+$/IFN-γ^+ T cells+$CD8^+$/TNF-α^+ T cells) to Tregs in the tumors treated with (1) LTX-315 or liposomal doxorubicin alone compared with those treated with RFH or control; (2) RFH+LTX-315 compared with those treated with LTX-315 alone; (3) RFH+liposomal doxorubicin compared with those treated with liposomal doxorubicin alone; (4) LTX-315+liposomal doxorubicin compared with those treated with LTX-315 or liposomal doxorubicin alone; and (5) RFH+LTX-315+liposomal doxorubicin compared with other seven treatment groups. These results further suggested that RFH could enhance the immunochemotherapeutic effect of LTX-315+liposomal doxorubicin through increasing the number of $CD8^+$ T cells and NK cells, and decreasing the number of Tregs, along with activating the function of $CD8^+$ T cells.

ELISA assay and qRT-PCR of Th1-type cytokines and Th2-type cytokines

As shown in figure 7, a significantly higher level of Th1-type cytokines in both plasma (IL-2, IL-12, IL-18, IFN-γ) and tumors (IL-2, IL-18, IFN-γ, TNF-α), as well as a

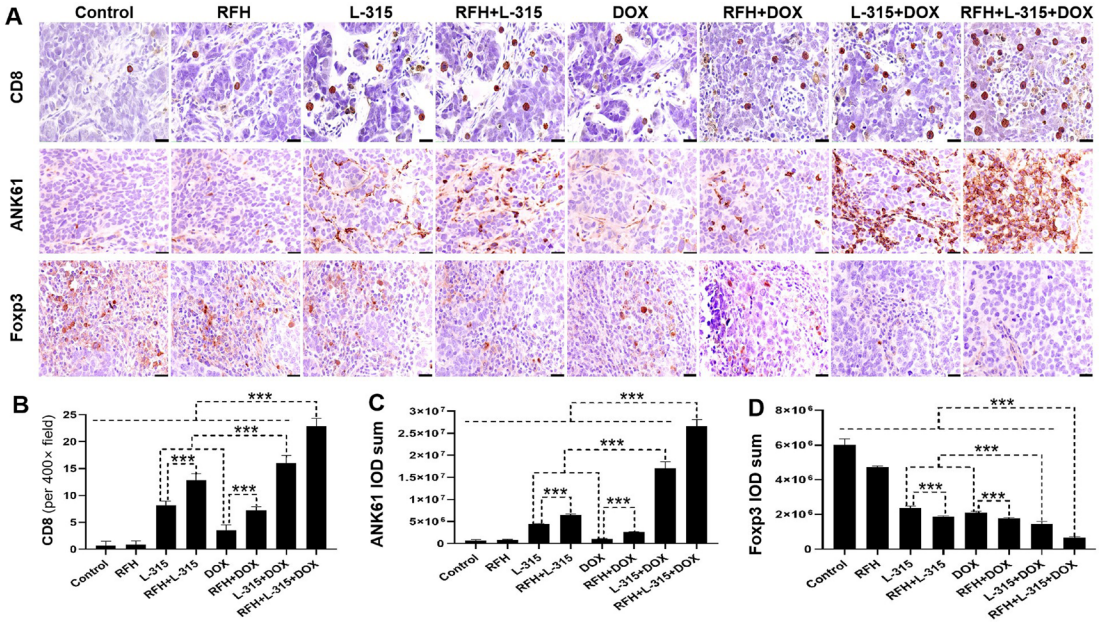

Figure 5 Immunohistochemical analysis of tumors among different treatment groups. (A with B, C) CD8 staining for CD8+T cells and ANK61 staining for natural killer (NK) cells in the treated tumors demonstrate a significantly higher number of CD8+ T cells and NK cells (brown color) in the triple combination treatment (RFH+LTX-315 (L-315)+DOX) group, compared with other seven treatment groups (***p<0.001). (A with D) The Foxp3 staining for regulatory T cells (Tregs, brown color) further confirms significantly decreased numbers of Tregs in the triple combination treatment, compared with other seven treatment groups (***p<0.001) (Scale bars, 20 µm). n=6 in each group. Error bars represent SD. RFH, radiofrequency hyperthermia.

significantly lower Th2-type cytokines of IL-4 and IL-10 in plasma and tumor were detected, when tumors treated with (1) LTX-315 or liposomal doxorubicin alone, compared with those treated with RFH or control; (2) RFH+LTX-315 compared with those treated with LTX-315 alone; (3) RFH+liposomal doxorubicin compared with those treated with liposomal doxorubicin alone; (4) LTX-315+liposomal doxorubicin compared with those treated with LTX-315 or liposomal doxorubicin alone; and (5) RFH+LTX-315+liposomal doxorubicin compared with other seven groups. These results provided further evidence on the immunotherapeutic effect of LTX-315 with liposomal doxorubicin, and the enhancement immunotherapeutic effect of RFH on LTX-315+liposomal doxorubicin for rat HCC.

DISCUSSION

Immunotherapy is a promising treatment method for HCC, but there are some barriers to immunotherapy for HCC, such as an immunosuppressive microenvironment.[33] Although immunotherapy has been shown to be effective in HCC, the response rates remain relatively low. For example, the CheckMate 459 trial, a randomized, open-label, multicenter, phase 3 trial study of an anti-programmed cell death protein-1 checkpoint inhibitor (nivolumab) versus sorafenib for patients with advanced HCC, demonstrated an objective response rate of only 14% in the group of nivolumab treatment, and nivolumab treatment did not significantly improve overall survival compared with sorafenib.[34] Some previous studies demonstrated that hyperthermia has immunomodulatory effects,[35 36] increases anticancers drug concentration in tumor cells,[37 38] and overcomes resistance mechanisms to immunotherapy in HCC.[33] The results of our study indicated RFH could enhance the immunotherapy for HCC.

To achieve a successful RFA of tumor, a >5 mm ablative margin around the entire tumor must be obtained. However, this is technically challenging to achieve such a safe margin for tumors larger than 3 cm and for those tumors located near large vessels or vital structures such as central bile ducts or gastrointestinal tract. In this study, we attempted to solve this critical clinical problem by integrating the advantages of the oncolytic peptide LTX-315, liposomal doxorubicin, and image-guided intratumoral RFH. The results of our study showed that (1) the combination of LTX-315 with liposomal doxorubicin has a better treatment effect in the treatment of rat HCC compared with LTX-315 or liposomal doxorubicin alone; and (2) intratumoral RFH further enhanced the treatment effect of LTX-315 in combination with liposomal doxorubicin.

The present study further elucidated the potential underlying biological mechanisms for such antitumor efficacy. The signal treatment with LTX-315 recruited and activated T cells, and the signal treatment with liposomal doxorubicin improved immunosuppressive microenvironment by reducing Tregs.[11 39] The two combined therapy of LTX-315 with liposomal doxorubicin or the triple combination treatment (RFH+LTX-315+liposomal doxorubicin) (1) significantly increased infiltration of

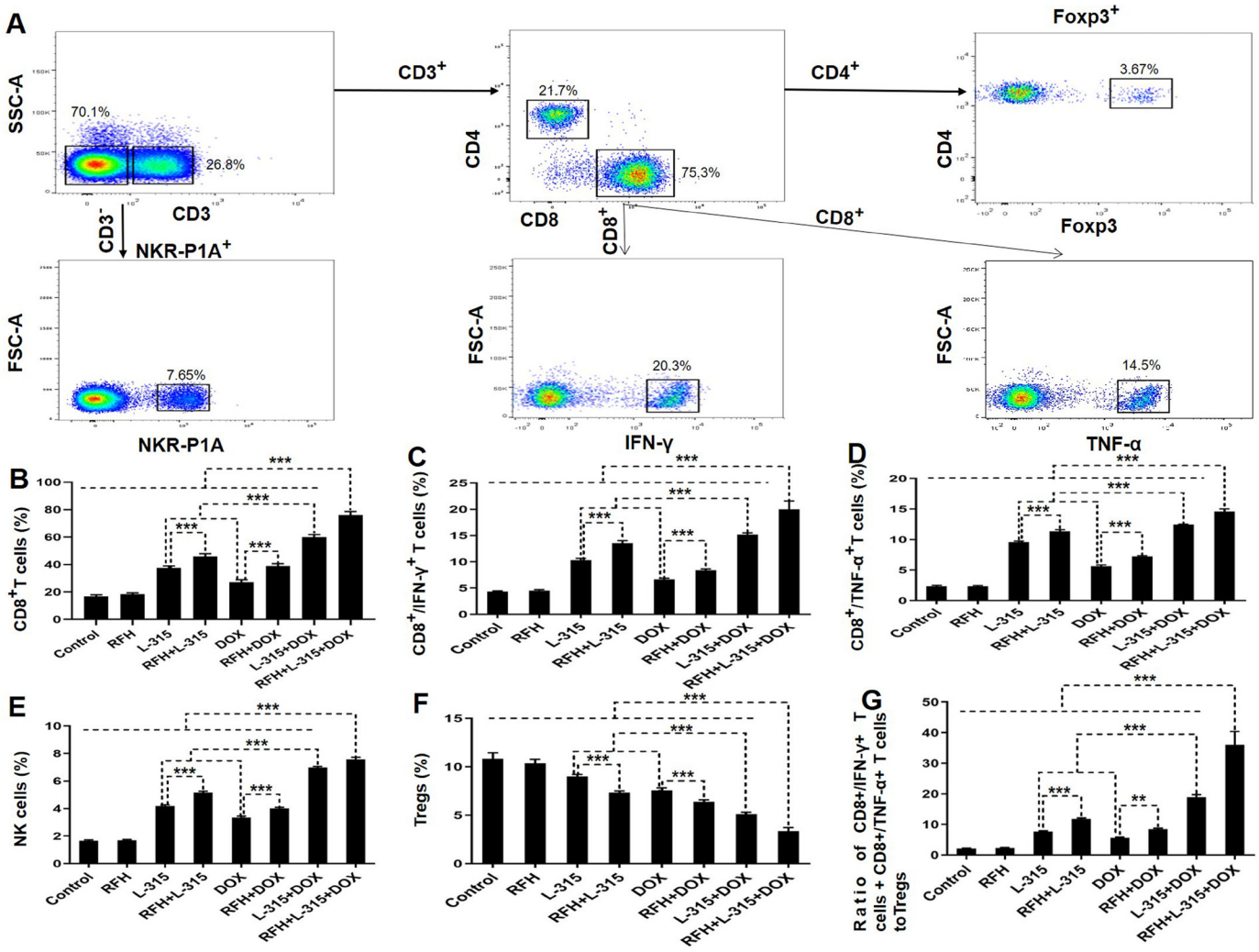

Figure 6 The percentages of different immune cells subtypes in tumor tissues among eight treatment groups. (A) Representative dot plots of the morphological characteristics (SSC vs FSC) exhibited by triple combination treated tumors (RFH+LTX-315 (L-315)+DOX). Schematic illustration of gating: Tumor-infiltrating lymphocytes determined by forward and side scatter properties, stained with relevant antibodies for flow cytometric analysis, to identify NK ($CD3^-$/$NKR\text{-}P1A^+$) cell and T ($CD3^+$/$NKR\text{-}P1A^-$) cell populations (including $CD4^+$ and $CD8^+$ T-cell subsets). The percentage of Tregs is derived from the percentage of $Foxp3^+$ cells within the total $CD4^+$ T-cell population. The percentage of $CD8^+$/IFN-γ^+ T cells or $CD8^+$/TNF-α^+ T cells is derived from the percentage of IFN-γ^+ or TNF-α^+ cells within the total $CD8^+$ T-cell population. Quantitative analysis further displays a significantly higher percentage of $CD8^+$ T cells, $CD8^+$/IFN-γ^+ T cells, $CD8^+$/TNF-α^+ T cells (B–D), and NK cells (E), a significantly lower percentage of Tregs (F), and a significantly higher ratio of pro-immune ($CD8^+$/IFN-γ^+ T cells+$CD8^+$/TNF-α^+ T cells) to Tregs (G) in the triple combination treatment group, compared with other seven treatment groups (**p<0.01, ***p<0.001). n=6 in each group. Error bars represent SD. FSC-A, forward scatter area; IFN, interferon; NK, natural killer; RFH, radiofrequency hyperthermia; SSC-A, side scatter area; TNF, tumor necrosis factor; Treg, regulatory T cells.

cytotoxic $CD8^+$ T cells and NK cells, and significantly decreased Tregs in the tumor bed, which altered the tumor microenvironment by turning 'cold' tumors into 'hot' tumors while converting the immunologically suppressive microenvironment from strong to weak; (2) significantly enhanced the immune function of $CD8^+$ T cells with more $CD8^+$/IFN-γ^+ T cells and $CD8^+$/TNF-α^+ T cells; and (3) significantly increased Th1-type cytokines to activate Th1-type response, and significantly decreased Th2-type cytokines to inhibit Th2-type response, which thus resulted in an effective antitumor effect.[40]

One of the primary disadvantages of systemic therapeutic administration is the insufficient dose of therapeutics delivered to the tumor targets, thus resulting in limited therapeutic efficacy with dose limiting toxicity for some patients. In the present study, we developed an innovative interventional oncology approach using image-guided local therapeutic/hyperthermia delivery to circumvent limitations of systemic administration of therapeutic agents.

In the present study, we directly delivered LTX-315 and /or liposomal doxorubicin to the tumors through multiple infusion prongs of the multipolar RFA electrode, which were precisely deployed under real-time ultrasound imaging guidance to ensure the full coverage of the tumor margin. Incomplete tumor ablation is

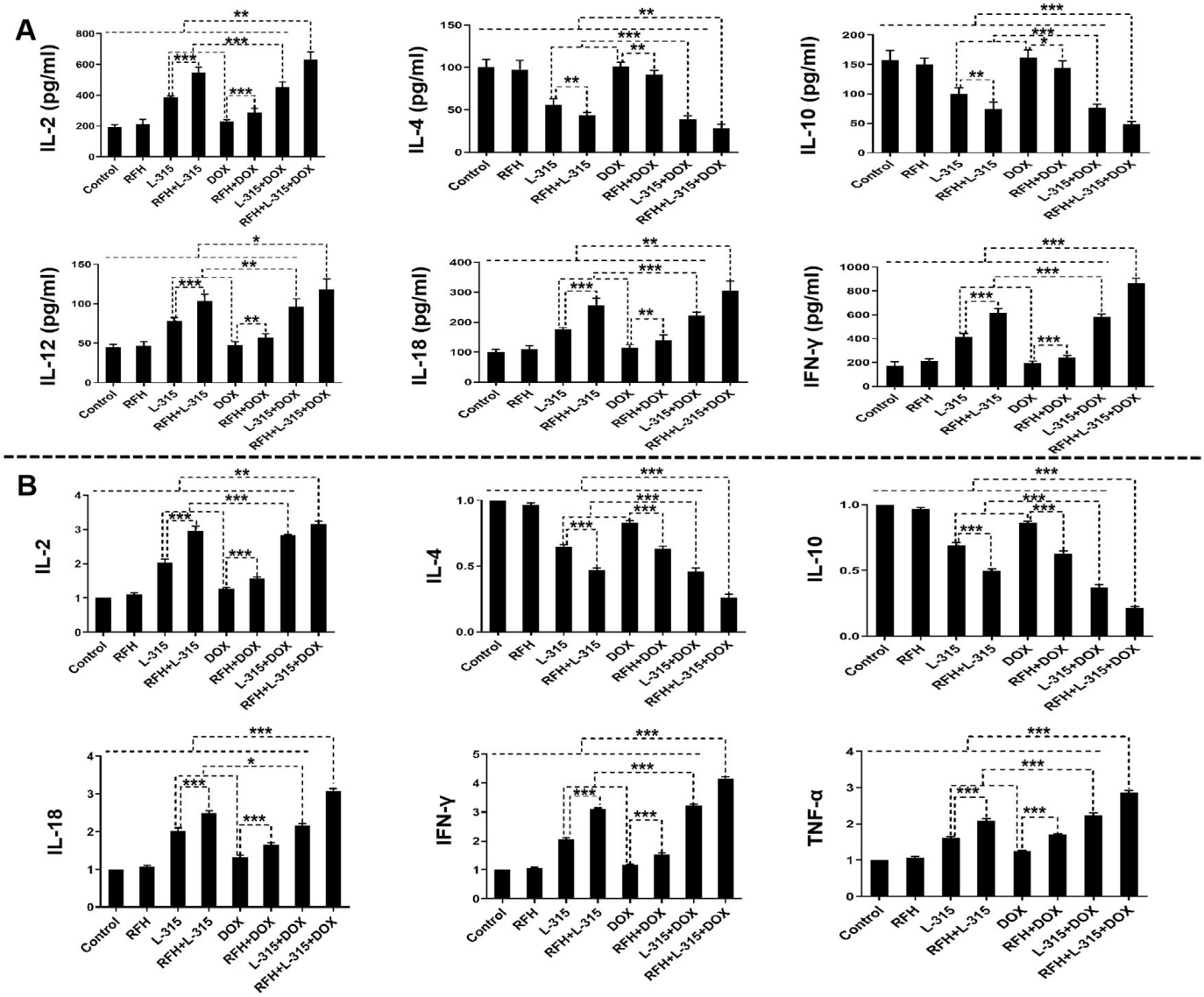

Figure 7 Quantitative analysis of Th1-type cytokines and Th2-type cytokines in plasma (A) and tumors (B), demonstrated a significant increase of Th1-type cytokines in plasma (IL-2, IL-12, IL-18, IFN-γ) and tumors (IL-2, IL-18, IFN-γ, TNF-α), as well as a significant decrease of Th2-type cytokines (IL-4, IL-10) in both plasma and tumors in the triple combination treatment group (RFH+LTX-315 (L-315)+DOX), compared with other seven treatment groups (*p<0.05, **p<0.01, ***p<0.001). n=6 in each group. Error bars represent SD. IFN, interferon; IL, interleukin; RFH, radiofrequency hyperthermia; TNF, tumor necrosis factor.

attributed to the challenge of creating an effective and safe ablation periphery with a 1 cm surgical margin or 'clear safety margin' beyond the tumor confinement.[41 42] The inability to obtain this clear margin is usually caused by thermal ablation heat carried away by blood flow when presence of larger neighboring vasculatures at the tumor periphery (so-called 'heat-sink' effect). This, in turn, generated a sublethal RFH at the margin of the ablated tumor during RFA. The sublethal RFH further enhanced the tumoricidal effect of LTX-315 in combination with liposomal doxorubicin by effectively facilitating the entrance of therapeutic agents into target tumor cells, and thereby promoting the destruction of tumor tissue. Therefore, the integration of image-guided RFH with the combined use of LTX-315 and liposomal doxorubicin may optimize formation of tumor-free margin during an RFA procedure and thus improve its efficacy especially for larger HCC.

Our study has limitations. Follow-up was only conducted for up to 2 weeks, and survival was not assessed because it was not permitted by our Institutional Animal Care and Use Committee.

In conclusion, the immunochemotherapy of LTX-315 with liposomal doxorubicin resulted in an excellent effect on HCC treatment by creating an antitumorigenic immunologic microenvironment. Image-guided intratumoral RFH can further enhance the treatment effect of LTX-315 in combination with liposomal doxorubicin for HCC. This novel concept may open new avenues for reducing the rates of residual and recurrent tumors after RFA of

medium-to-large HCCs, which leads to explore further studies on clinical applications of this concept and efficacy on other types of malignancy.

Author affiliations
[1]Image-Guided Bio-Molecular Intervention Research and Section of Vascular and Interventional Radiology, Department of Radiology, University of Washington School of Medicine, Seattle, Washington, USA
[2]Department of Radiology, Union Hospital, Tongji Medical College, Huazhong University of Science and Technology, Wuhan, China
[3]Hepatobiliary and Pancreatic Interventional Treatment Center, Division of Hepatobiliary and Pancreatic Surgery, Zhejiang University School of Medicine First Affiliated Hospital, Hangzhou, China
[4]Department of Pathology, Overlake Medical Center and Incyte Diagnostics, Bellevue, WA, USA

Contributors XY and CZ designed research; XK and GZ performed the experiments, XK, GZ, FZ, and XY analyzed the data; XK, GZ, FZ, HJ, DSS, WM, CZ, and XY wrote the paper. XY and CZ were responsible for supervision and the overall content as the guarantors.

Funding This study was supported by the grants of NIH R01EB028095 and National Natural Science Foundation of China (No. 82072041).

Competing interests None declared.

Patient consent for publication Not applicable.

Ethics approval Not applicable.

Provenance and peer review Not commissioned; externally peer reviewed.

Data availability statement Data are available upon reasonable request.

ORCID iD
Xiaoming Yang http://orcid.org/0000-0002-4076-3569

REFERENCES

1 Kim G-A, Shim JH, Kim M-J, *et al*. Radiofrequency ablation as an alternative to hepatic resection for single small hepatocellular carcinomas. *Br J Surg* 2016;103:126–35.
2 Young S, Golzarian J. Locoregional therapies in the treatment of 3- to 5-cm hepatocellular carcinoma: critical review of the literature. *AJR Am J Roentgenol* 2020;215:223–34.
3 Chen Q-W, Ying H-F, Gao S, *et al*. Radiofrequency ablation plus chemoembolization versus radiofrequency ablation alone for hepatocellular carcinoma: a systematic review and meta-analysis. *Clin Res Hepatol Gastroenterol* 2016;40:309–14.
4 Yuan H, Liu F, Li X, *et al*. Transcatheter arterial chemoembolization combined with simultaneous DynaCT-guided radiofrequency ablation in the treatment of solitary large hepatocellular carcinoma. *Radiol Med* 2019;124:1–7.
5 European Association for the Study of the Liver. Electronic address: easloffice@easloffice.eu, European Association for the Study of the Liver. EASL clinical practice guidelines: management of hepatocellular carcinoma. *J Hepatol* 2018;69:182–236.
6 Ikeda M, Mitsunaga S, Ohno I, *et al*. Systemic chemotherapy for advanced hepatocellular carcinoma: past, present, and future. *Diseases* 2015;3:360–81.
7 Gabizon AA, Patil Y, La-Beck NM. New insights and evolving role of pegylated liposomal doxorubicin in cancer therapy. *Drug Resist Updat* 2016;29:90–106.
8 Theodoulou M, Hudis C. Cardiac profiles of liposomal anthracyclines: greater cardiac safety versus conventional doxorubicin? *Cancer* 2004;100:2052–63.
9 Abu Eid R, Razavi GSE, Mkrtichyan M, *et al*. Old-School chemotherapy in immunotherapeutic combination in cancer, a low-cost drug repurposed. *Cancer Immunol Res* 2016;4:377–82.
10 Alizadeh D, Trad M, Hanke NT, *et al*. Doxorubicin eliminates myeloid-derived suppressor cells and enhances the efficacy of adoptive T-cell transfer in breast cancer. *Cancer Res* 2014;74:104–18.
11 Fucikova J, Kralikova P, Fialova A, *et al*. Human tumor cells killed by anthracyclines induce a tumor-specific immune response. *Cancer Res* 2011;71:4821–33.
12 Zongyi Y, Xiaowu L. Immunotherapy for hepatocellular carcinoma. *Cancer Lett* 2020;470:8–17.
13 Johnston MP, Khakoo SI. Immunotherapy for hepatocellular carcinoma: current and future. *World J Gastroenterol* 2019;25:2977–89.
14 Jiang Y, Han Q-J, Zhang J. Hepatocellular carcinoma: mechanisms of progression and immunotherapy. *World J Gastroenterol* 2019;25:3151–67.
15 Greten TF, Wang XW, Korangy F. Current concepts of immune based treatments for patients with HCC: from basic science to novel treatment approaches. *Gut* 2015;64:842–8.
16 Prieto J, Melero I, Sangro B. Immunological landscape and immunotherapy of hepatocellular carcinoma. *Nat Rev Gastroenterol Hepatol* 2015;12:681–700.
17 Yang T, Yu S, Liu L, *et al*. Dual polymeric prodrug co-assembled nanoparticles with precise ratiometric co-delivery of cisplatin and metformin for lung cancer chemoimmunotherapy. *Biomater Sci* 2020;8:5698–714.
18 Wang H, Xuan T-T, Chen Y, *et al*. Investigative therapy for advanced esophageal cancer using the option for combined immunotherapy and chemotherapy. *Immunotherapy* 2020;12:697–703.
19 Yhim H-Y, Yoon DH, Kim SJ, *et al*. First-line treatment for primary breast diffuse large B-cell lymphoma using immunochemotherapy and central nervous system prophylaxis: a multicenter phase 2 trial. *Cancers* 2020;12:2192.
20 Camilio KA, Berge G, Ravuri CS, *et al*. Complete regression and systemic protective immune responses obtained in B16 melanomas after treatment with LTX-315. *Cancer Immunol Immunother* 2014;63:601–13.
21 Nestvold J, Wang M-Y, Camilio KA, *et al*. Oncolytic peptide LTX-315 induces an immune-mediated abscopal effect in a rat sarcoma model. *Oncoimmunology* 2017;6:e1338236.
22 Zhang F, Le T, Wu X, *et al*. Intrabiliary RF heat-enhanced local chemotherapy of a cholangiocarcinoma cell line: monitoring with dual-modality imaging--preclinical study. *Radiology* 2014;270:400–8.
23 Shi Y, Zhang F, Bai Z, *et al*. Orthotopic esophageal cancers: intraesophageal hyperthermia-enhanced direct chemotherapy in rats. *Radiology* 2017;282:103–12.
24 Zhu L, Xu Y, Shan Y, *et al*. Intraperitoneal perfusion chemotherapy and whole abdominal hyperthermia using external radiofrequency following radical D2 resection for treatment of advanced gastric cancer. *Int J Hyperthermia* 2019;36:402–6.
25 Zheng H, Zhang F, Monsky W, *et al*. Interventional optical Imaging-Monitored synergistic effect of radio-frequency hyperthermia and oncolytic immunotherapy. *Front Oncol* 2021;11:821838.
26 Li Z, Deng J, Sun J, *et al*. Hyperthermia targeting the tumor microenvironment facilitates immune checkpoint inhibitors. *Front Immunol* 2020;11:595207.
27 Antanavičiūtė I, Mildažienė V, Stankevičius E, *et al*. Hyperthermia differently affects connexin43 expression and gap junction permeability in skeletal myoblasts and HeLa cells. *Mediators Inflamm* 2014;2014:1–16.
28 Song J, Zhang F, Ji J, *et al*. Orthotopic hepatocellular carcinoma: molecular imaging-monitored intratumoral hyperthermia-enhanced direct oncolytic virotherapy. *Int J Hyperthermia* 2019;36:343–9.
29 Choi JW, Kim JH, Kim H-C, *et al*. Comparison of tumor vascularity and hemodynamics in three rat hepatoma models. *Abdom Radiol* 2016;41:257–64.
30 Lee TK, Na KS, Kim J, *et al*. Establishment of animal models with orthotopic hepatocellular carcinoma. *Nucl Med Mol Imaging* 2014;48:173–9.
31 Li L, Guo X, Peng X, *et al*. Radiofrequency-responsive dual-valent gold nanoclusters for enhancing synergistic therapy of tumor ablation and artery embolization. *Nano Today* 2020;35:100934.

32 Li G, Ye L, Pan J, *et al*. Antitumoural hydroxyapatite nanoparticles-mediated hepatoma-targeted trans-arterial embolization gene therapy: in vitro and in vivo studies. *Liver Int* 2012;32:998–1007.
33 Muñoz NM, Dupuis C, Williams M, *et al*. Immune modulation by molecularly targeted photothermal ablation in a mouse model of advanced hepatocellular carcinoma and cirrhosis. *Sci Rep* 2022;12:14449.
34 Yau T, Park J-W, Finn RS, *et al*. Nivolumab versus sorafenib in advanced hepatocellular carcinoma (CheckMate 459): a randomised, multicentre, open-label, phase 3 trial. *Lancet Oncol* 2022;23:77–90.
35 Li Z, Deng J, Sun J, *et al*. Hyperthermia targeting the tumor microenvironment facilitates immune checkpoint inhibitors. *Front Immunol* 2020;11:595207.
36 Chen P-M, Pan W-Y, Wu C-Y, *et al*. Modulation of tumor microenvironment using a TLR-7/8 agonist-loaded nanoparticle system that exerts low-temperature hyperthermia and immunotherapy for in situ cancer vaccination. *Biomaterials* 2020;230:119629.
37 Qian K, Chen M, Zhang F, *et al*. Image-Guided Radiofrequency Hyperthermia (RFH)-Enhanced Direct Chemotherapy of Hepatic Tumors: The Underlying Biomolecular Mechanisms. *Front Oncol* 2020;10:610543.
38 Ji J, Weng Q, Zhang F, *et al*. Non-Small-Cell lung cancer: feasibility of intratumoral radiofrequency hyperthermia-enhanced herpes simplex virus thymidine kinase gene therapy. *Radiology* 2018;288:612–20.
39 Camilio KA, Wang M-Y, Mauseth B, *et al*. Combining the oncolytic peptide LTX-315 with doxorubicin demonstrates therapeutic potential in a triple-negative breast cancer model. *Breast Cancer Res* 2019;21:9.
40 Li L, Wang W, Pan H, *et al*. Microwave ablation combined with OK-432 induces Th1-type response and specific antitumor immunity in a murine model of breast cancer. *J Transl Med* 2017;15:23.
41 Schaible J, Pregler B, Bäumler W, *et al*. Safety margin assessment after microwave ablation of liver tumors: inter- and intrareader variability. *Radiol Oncol* 2020;54:57–61.
42 Shady W, Petre EN, Do KG, *et al*. Percutaneous Microwave versus Radiofrequency Ablation of Colorectal Liver Metastases: Ablation with Clear Margins (A0) Provides the Best Local Tumor Control. *J Vasc Interv Radiol* 2018;29:268–75.